RSC Sustainability

ROYAL SOCIETY OF CHEMISTRY

PAPER

View Article Online
View Journal | View Issue

Cite this: *RSC Sustainability*, 2024, **2**, 2267

Catalytic synthesis of renewable 2-methylfuran from furfural†

Yuanyuan Han,[a] Xing Zhang,[a] Wei Wang,[a] Shaobo Guo,[a] Xiaohui Ji*[a] and Guangyi Li*[b]

Received 11th May 2024
Accepted 29th May 2024

DOI: 10.1039/d4su00229f

rsc.li/rscsus

Biomass energy stands at the forefront of remedial strategies for the current energy deficit and has garnered considerable attention. The deployment of highly efficient catalysts is pivotal to the success of this energy form. Prevailing literature established that high-valent metal presence contributed significantly to the hydrogenation of furfural to prepare 2-methylfuran. In this study, we elucidated the efficacy of a monometallic catalyst consisting solely of cobalt and its oxides, denoted as Co/CoO_x, in the catalytic transformation of furfural derived from lignocellulosic biomass into 2-methylfuran. Leveraging the economical Co/CoO_x catalyst, in conjunction with minimal addition of hydroquinone, we accomplished the selective hydrodeoxygenation of furfural, culminating in an augmented yield of 2-MF up to 73%. This investigation is the inaugural confirmation that minuscule quantities of hydroquinone can efficaciously mitigate side reactions such as the polymerization of furfural within the selective hydrodeoxygenation process. The Co/CoO_x catalyst was characterized through an array of analytical techniques, including XRD, H_2-TPR and N_2-adsorption. These characterization studies unveiled that the optimal selectivity for 2-methylfuran was achieved when the ratio of Co^0 : Co^{2+} in the catalyst approached approximately 95%.

Sustainability spotlight

The fuels derived from non-edible lignocellulosic biomass were referred to as second-generation biomass hydrocarbon fuels, representing an optimal low-carbon alternative to conventional fossil fuels. A significant impediment to the widespread deployment of second-generation biomass hydrocarbon fuel is its elevated production expenses. Presently, furfural stands as one of the most extensively produced lignocellulosic derivatives on an annual basis, with 2-methylfuran playing a pivotal role in the synthesis of second-generation biomass fuels. This research employed an economical cobalt-based catalyst to enable the efficient catalytic transformation of furfural into 2-methylfuran, laying the foundation for the cost-effective production of 2-methylfuran in the future, thus contributing to a decrease in the manufacturing expenses of second-generation biofuels.

1 Introduction

In the contemporary period, scholarly attention has increasingly concentrated on the technological progress in transforming biomass and its derivatives into liquid biofuels and bulk chemicals.[1–4] Within this domain, the processes of biomass refining and upgrading have surfaced as pivotal fields of inquiry. A salient intermediate, furfural, originating from lignocellulosic biomass, has elicited significant interest from the research community.[5,6] Furfural exhibited the potential to be efficiently converted into a multitude of high-value chemicals, such as 2-methylfuran (2-MF),[7] 2-methyltetrahydrofuran,[8,9] and furfuryl alcohol,[10–12] through the application of various catalysts under diverse reaction conditions. The production of 2-MF from furfural has attracted widespread attention because it can serve as a fuel in its own right[13] and is also a key intermediate in the preparation of renewable aviation kerosene or diesel.[14]

2-MF can be synthesized through various chemical reactions, with the selective hydrodeoxygenation of furfural being the most extensively examined route for its production. Historically, the generation of 2-MF utilized the catalytic oxidation of 1,4-pentadiene.[15] Nonetheless, the refinement of furfural production processes has led to the evolution of more efficient synthetic methodologies. In the year 1947, Bremenr *et al.*[16] pioneered the development of CuAl and CuCr catalysts, with magnesium serving as a promoter. Employed at reaction temperatures of around 250 °C, these catalysts predominantly yielded 2-MF. Notably, CuCr catalysts demonstrated exceptional selectivity towards 2-MF, consistently delivering yields in excess of 85% within a temperature spectrum of 200 °C to 300 °C. Subsequent comparative

[a]*Shaanxi Key Laboratory of Catalysis, School of Chemical & Environment Science, Shaanxi University of Technology, Hanzhong, Shaanxi 723001, P. R. China. E-mail: jixiaohui@snut.edu.cn*

[b]*CAS Key Laboratory of Science and Technology on Applied Catalysis, Dalian Institute of Chemical Physics, Chinese Academy of Sciences, Dalian 116023, China. E-mail: lgy2010@dicp.ac.cn*

† Electronic supplementary information (ESI) available. See DOI: https://doi.org/10.1039/d4su00229f

studies of CuZnAl, CuMgAl, $Cu_2Cr_2O_5$, and CuNiAl catalysts for the gas-phase selective hydrodeoxygenation of furfural were conducted by Ma *et al.*[17] Their findings indicated that $Cu_2Cr_2O_5$ catalysts afforded superior selectivity for 2-MF, with a yield of 73.5% being attained at 240 °C. Nevertheless, owing to the toxicological concerns associated with chromium, there was a concerted effort within the research community to identify environmentally benign alternatives to chromium-based catalysts in the pursuit of green chemical processes.[18]

In the domain of synthesizing 2-MF through the selective hydrodeoxygenation of furfural, scholarly investigations have revealed that noble metal catalysts exhibited superior selective hydrodeoxygenation performance. For example, Aldosari *et al.*[19] synthesized a 4%Pd–1%Ru/TiO_2 catalyst, achieving a 51.5% yield of 2-MF under ambient conditions. Vlachos *et al.*[20] utilized a Ru/C catalyst to facilitate selective hydrodeoxygenation, culminating in a 76% yield of 2-MF after a reaction duration of 10 hours at a temperature of 180 °C, employing 2-pentanol as the reaction medium. In another notable study, Date *et al.*[21] reported a 95% yield of 2-MF using an Ir/C catalyst at a reaction temperature of 220 °C, attributing this enhanced yield to the abundance of acidic sites on the catalyst provided by the presence of iridium oxide. Despite these advancements, the broader industrial application of such catalysts was constrained by factors including the availability and cost of noble metals.

Catalysts composed of non-precious metals were extensively employed in the selective hydrodeoxygenation of furfural, favored for their cost-effectiveness and reduced environmental footprint. Among them, copper-based catalysts were distinguished for their superior catalytic performance and were supported by relatively plentiful reserves. Xu *et al.*[22] successfully synthesized a copper-based catalyst utilizing a CuMgAlNi hydrotalcite-like precursor and examined the implications of varied reduction temperatures on the selective hydrodeoxygenation process of furfural. The research findings indicated that at a reduction temperature of 300 °C, the gaseous-phase catalytic selective hydrodeoxygenation of furfural predominantly generated 2-MF, achieving a selectivity of 48%. An escalation in the reduction temperature was observed to inversely affect the selectivity towards 2-MF, while concurrently augmenting the selectivity for furfuryl alcohol. This phenomenon underscored the significant role of copper particle size in dictating the selectivity of the selective hydrodeoxygenation reaction. Moreover, the incorporation of cobalt has been shown to augment the catalytic efficacy of copper-based catalysts. Kalong *et al.*[23] employed a wet impregnation technique to synthesize both monometallic Cu/γ-Al_2O_3 and bimetallic CuCo/γ-Al_2O_3 catalysts, subsequently evaluating their catalytic performance. The findings of the study suggested that the bimetallic catalysts exhibited an alloyed state, which served to bolster their capacity for C–O bond cleavage, thereby advancing the selectivity toward 2-MF. Despite these advancements, such catalysts were encumbered by limitations including elevated reaction temperatures, protracted durations of reaction, and suboptimal substrate-to-catalyst ratios. Consequently, there existed a critical imperative to devise a catalyst that was not only environmentally benign and cost-efficient but also exhibited superior performance in the conversion of furfural to 2-MF, with the aim of achieving high product yields.

Notably, in recent years, the Cu/AC catalyst disclosed by Gong *et al.*[24] achieved nearly 100% yield of 2-MF. Likewise, Li *et al.*[25] reported that the Ni–Cu/C catalyst attained a high yield of 98% of 2-MF. The Co–Cu/ZrO_2 catalyst reported by Akmaz *et al.*[26] achieved a 94.1% yield of 2-MF at 200 °C. Moreover, the Co-CoO_x/AC catalyst, as reported by Zhang *et al.*,[27] stood out for operating at the lowest reaction temperature, as low as 120 °C, yet yielding 87.4% of 2-MF (see Table 1). It was worth noting that the presence of a certain proportion of metal oxides in the catalyst contributed to achieving high yields of 2-MF. For example, in the Cu/AC catalyst, a desired ratio of $Cu^0 : Cu^+ : Cu^{2+}$ efficiently catalyzed the conversion of furfural to 2-MF. An *et al.*[28] confirmed that the addition of Mo in the Cu–Mo/CoO_x catalyst promoted the formation of the CuCo alloy and $Co^{\delta+}$ species, which were beneficial for the adsorption of furfural and catalytic cleavage of C–O bonds. The Co-CoO_x/AC catalyst has also been confirmed to simultaneously contain Co^0 and Co^{2+}. It can be observed that a certain proportion of high-valent metal presence contributed significantly to the hydrogenation of furfural to prepare 2-MF. However, due to the presence of carriers or the interaction of the second metal with metal oxides, it's challenging to quantitatively describe the content of high-valent metals in the catalysts mentioned above.

Recently, Xiang *et al.*[29] elucidated the efficient catalytic capability of the Co@CoO catalyst in the conversion of 5-hydroxymethylfurfural to 2,5-dimethylfuran. This monometallic catalyst, comprising solely a metal and its corresponding oxides, facilitated the precise determination of the metal-to-metal oxide ratio. The present investigation was centred on the catalytic transformation of furfural over a Co/CoO_x catalyst, which has been shown to facilitate the efficient conversion of furfural to 2-MF. Through the modulation of the reduction temperature, it was possible to convert pristine Co_3O_4 into an active composite consisting of metallic Co and CoO_x, collectively referred to as Co/CoO_x, which was confirmed through characterization analysis of its composition and structural features. Reaction conditions of 170 °C, a reaction duration of 2 hours, and a pressure of 2 MPa, coupled with trace amounts of hydroquinone, culminated in a notable yield of 73% for 2-MF. It is obvious that the Co/CoO_x catalyst used in this study is a non-precious metal catalyst that can efficiently achieve a high yield of 2-MF when the furfural/catalyst ratio was 10 : 1. This work posited a simplified mechanistic route for the conversion process of furfural to 2-MF, augmenting our understanding of the underlying chemical processes. Additionally, employing H_2-TPR, the ratio of $Co^0 : Co^{2+}$ in the catalyst was quantitatively described, observing that the optimal selectivity for 2-MF was achieved when this ratio approached approximately 95%.

2 Materials and methods

2.1 Materials

Furfural (99.0%), furfuryl alcohol (99.0%), tetrahydrofurfuryl alcohol (THFA, 99.0%), 2-methylfuran (2-MF, 99.0%), 2,5-dimethylfuran (99.0%), and hydroquinone

Table 1 List of non-precious metal catalysts using hydrogen reduction to catalyze furfural to 2-MF

Entry	Catalyst	T (°C)	2-MF yield (%)	Time (h)	Furfural to catalyst ratio	Ref.
1	Cu/AC	170	100	4	1 : 1	24
2	NiCu/C	220	98	5	10 : 1	25
3	Co–Cu/ZrO_2	200	94.1	6	5 : 2	26
4	Cu–Co/γ-Al_2O_3	180	94	3.5	8 : 1	23
5	NiCo–MgAlO	220	92.1	6	6 : 1	42
6	Cu_3–Mo_1/CoO_x	180	92	4	13 : 4	28
7	Co–CoO_x/AC	120	87.4	5	10 : 1	27
8	Cu–Co/Al_2O_3	220	87	5	7 : 3	43
9	$Cu_2Cr_2O_5$	240	73.5	5	1 : 1	15
10	CuCo/γ-Al_2O_3	200	50	6	10 : 1	21
11	CuMgAlNi	300	48	2	5 : 1	20
12	W_xC/SiO_2	200	45	24	7 : 1	44
13	Co/CoO_x	170	73	2	10 : 1	This work

(99.0%) were purchased from Shanghai Aladdin Biochemical Technology Co., Ltd. Isopropanol (99.0%) was purchased from Guangdong Guanghua Sci-Tech Co., Ltd. Analytical grade cobalt nitrate hexahydrate and ammonium carbonate were purchased from Xilong Scientific Co., Ltd. Except for furfural and furfuryl alcohol, which were pretreated by vacuum distillation before use, no other reagents were treated.

2.2 Catalyst synthesis

A precipitation method was used to synthesize Co/CoO_x, in which cobalt nitrate was used as a precursor for synthesis.[29] In a typical procedure, 60 mmol of cobalt nitrate and 69 mmol of $(NH_4)_2CO_3$ were dissolved separately in 200 mL of distilled water, and the $(NH_4)_2CO_3$ solution was added dropwise into the cobalt nitrate solution with vigorous stirring. The resulting suspension was aged with stirring at 60 °C for 1 h and allowed to stand at room temperature for 12 h. After filtration and washing with distilled water, the solid product was dried at 100 °C for 12 h and finally calcined in air at 450 °C for 4 h to obtain the desired Co/CoO_x sample precursor.

The prepared Co/CoO_x precursor was further reduced in a tube furnace under H_2 (10% H_2–Ar mixed gas) at the desired temperature (200–350 °C) with a heating rate of 2 °C min^{-1} for 2 h. The resulting reduced cobalt oxide was labeled as Co/CoO_x-m, where m represents the reduction temperature.

Table 2 Structural characteristics of Co/CoO_x at different reduction temperatures[a]

Reduction temperature (°C)	BET surface area (m^2 g^{-1})	Total pore volume (cm^3 g^{-1})
200 °C	25.7	0.010
250 °C	6.1	0.0024
300 °C	5.8	0.0021
350 °C	3.4	0.0012

[a] Note: 200 °C represents Co/CoO_x reduced at 200 °C; 250 °C represents Co/CoO_x reduced at 250 °C; 300 °C represents Co/CoO_x reduced at 300 °C; 350 °C represents Co/CoO_x reduced at 350 °C.

2.3 Catalytic activity testing in a batch reactor

The selective hydrodeoxygenation of furfural was conducted in a 100 mL stainless steel high-pressure reactor. The required amount of furfural, catalyst, and solvent was sealed in the reactor, which was then purged three times with N_2 and H_2 respectively to remove air and fill in the desired H_2 pressure. The reactor was rapidly heated to the predetermined temperature, and after the reaction, it was cooled in an ice bath. The reaction liquid was filtered through a 13 mm × 0.22 μm organic membrane filter for product analysis. Qualitative analysis was performed using a gas chromatography-mass spectrometry system (QP2020 NX), and quantitative analysis was conducted using a gas chromatography system (Agilent 7890B) equipped with an HP-5 column and an FID detector. The carrier gas type of gas chromatography is helium.

The conversion of furfural and the yield of products were calculated using 2,5-dimethylfuran as an internal standard, based on the product yield.

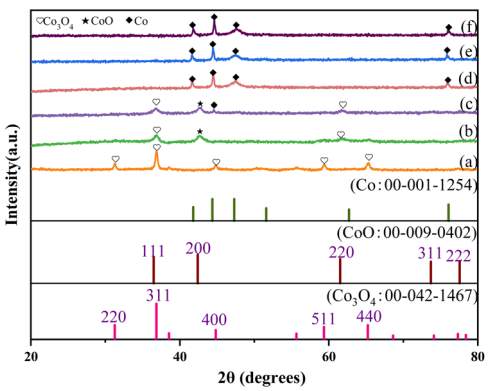

Fig. 1 XRD patterns of (a) unreduced Co/CoO_x, (b) 200 °C reduced Co/CoO_x, (c) 250 °C reduced Co/CoO_x, (d) 300 °C reduced Co/CoO_x and (e) 350 °C reduced Co/CoO_x.

Table 3 The atomic ratio of Co atoms with different valence states in Co/CoO_x catalysts

Reduction temperature[a] (°C)	Quantity[b] (mmol g^{-1})	Atomic ratio[c]
200 °C	16.06	$Co^{2+}:Co^{3+}=69.7\%:30.3\%$
250 °C	1.872	$Co^{0}:Co^{2+}=84.9\%:15.1\%$
300 °C	0.875	$Co^{0}:Co^{2+}=94.8\%:5.2\%$
350 °C	0.801	$Co^{0}:Co^{2+}=95.2\%:4.8\%$

[a] 200 °C represents Co/CoO_x reduced at 200 °C; 250 °C represents Co/CoO_x reduced at 250 °C; 300 °C represents Co/CoO_x reduced at 300 °C; 350 °C represents Co/CoO_x reduced at 350 °C. [b] Hydrogen consumption in the H_2-TPR test. [c] The atomic ratio of Co atoms with different valence states calculated from the hydrogen consumption in H_2-TPR.

$$\text{Conversion (\%)} = [(\text{Moles of reacted furfural})/(\text{Moles of initial furfural})] \times 100 \quad (1)$$

$$\text{Yield (\%)} = [(\text{Moles of product})/(\text{Moles of initial furfural})] \times 100 \quad (2)$$

2.4 Catalyst characterization

The crystal structure information of the catalyst was determined using an Empyrean-100 X-ray diffractometer from the Dutch company PANalytical. The instrument was operated at a scanning speed of 10° min^{-1} in the range of 10–80°, with a Cu Kα radiation source ($\lambda = 0.15432$ nm), a tube voltage of 40 kV, and a tube current of 40 mA.

The specific surface area, average pore size, and pore volume of the catalyst were determined using a Micromeritics ASAP 2460 physical adsorption analyzer. Prior to the analysis, the sample was pretreated at 110 °C under vacuum for one hour, followed by a 6 h degassing at 350 °C to remove various gases and impurities adsorbed on the catalyst surface. The N_2 adsorption–desorption measurement was conducted at 77 K liquid nitrogen temperature under a vacuum pressure of 10^{-6} torr. The specific surface area was calculated using the BET equation after completion of the analysis. The method adopted for calculating the aperture distribution is the Barrett–Joyner–Halenda method.

The H_2-TPR (hydrogen temperature programmed reduction) technique on an Autochem II 2920 chemisorption analyzer from Micromeritics was used to characterize the differences in reduction temperatures of various catalysts. First, the samples were pretreated at 400 °C in an Ar atmosphere for 30 minutes to remove surface-adsorbed impurities. The samples were then cooled to 50 °C and the carrier gas was switched to a 10 vol% H_2/Ar mixed gas. After the baseline had stabilized, the samples were heated from 50 °C to 800 °C at a rate of 10 °C min^{-1}. A thermal conductivity detector (TCD) was used to record the test signal throughout the process, and a cold trap was installed before the TCD to remove water produced during the reduction process.

3 Results and discussion

3.1 Catalyst characterization

To investigate the influence of the reduction process on the catalyst structure, the specific surface area and pore structure of the catalyst were characterized. As shown in Fig. S1,† the N_2 adsorption–desorption isotherms for Co/CoO_x at varying temperatures of reduction displayed characteristics of type IV isotherms, indicative of the presence of mesoporous structures within the materials.[30] Table 2 presents the BET specific surface area and pore volume data. Specifically, the Co/CoO_x-200 sample exhibited a specific surface area of 25.7 m^2 g^{-1} and a pore volume of 0.01 cm^3 g^{-1}. A discernible trend was observed

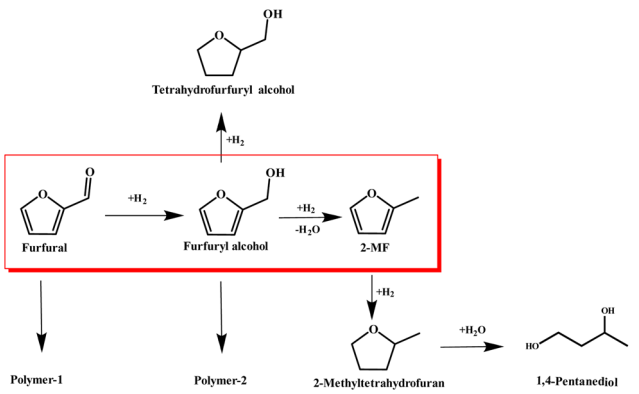

Scheme 1 The pathway for the selective hydrodeoxygenation of furfural.

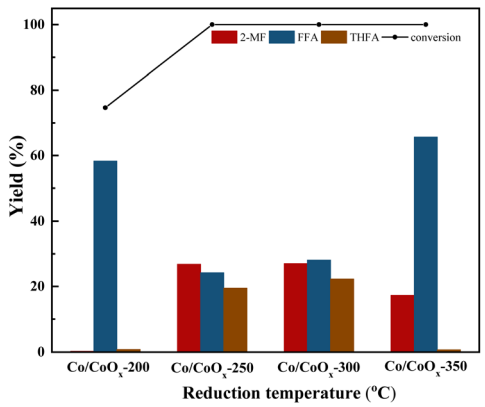

Fig. 2 Effect of reduction temperature on furfural selective hydrodeoxygenation conversion and yield using Co/CoO_x catalysts. Reaction conditions: furfural 2 g, isopropyl 40 mL, catalyst 200 mg, agitation speed 700 rpm, H_2 pressure 2 MPa, temperature 130 °C, time 2 h. 2-MF: 2-methylfuran, FFA: furfuryl alcohol, THFA: tetrahydrofurfuryl alcohol.

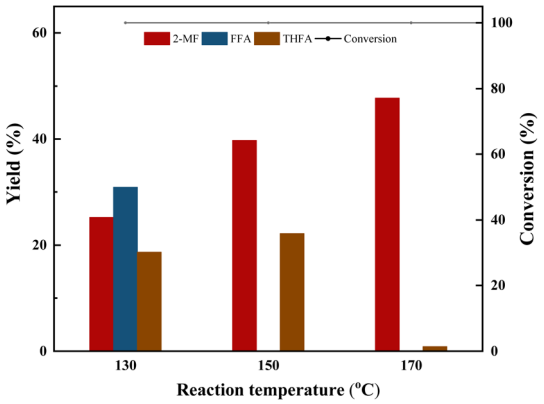

Fig. 3 Effect of reaction temperature on furfural selective hydrodeoxygenation conversion and yield using Co/CoO_x-300 catalysts. Reaction conditions: furfural 2 g, isopropyl 40 mL, catalyst 200 mg, agitation speed 700 rpm, H_2 pressure 2 MPa, time 2 h. 2-MF: 2-methylfuran, FFA: furfuryl alcohol, THFA: tetrahydrofurfuryl alcohol.

wherein an elevation in the reduction temperature resulted in a concomitant decrease in the catalyst's specific surface area, which diminished to 3.4 $m^2\ g^{-1}$, and the pore volume concurrently contracted to 0.0012 $cm^3\ g^{-1}$. This reduction in surface area and pore volume may be attributed to the collapse of pores during the reduction process.[31]

XRD analysis was also used to characterize the phases of these catalysts (Fig. 1). For unreduced Co/CoO_x, only the spinel phase Co_3O_4 was observed. The main spinel phases of Co/CoO_x-200 were Co_3O_4 and a small amount of cubic phase CoO. The XRD pattern of Co/CoO_x-250 showed a mixture of cubic phases of Co, CoO and Co_3O_4. Co/CoO_x-300 and Co/CoO_x-350 mainly exhibited a metallic Co structure. Five significant diffraction peaks were observed in the XRD pattern for Co_3O_4 at $2\theta = 31.2°$, 36.8°, 44.8°, 59.3°, and 65.2°, corresponding to the (220), (311), (400), (511), and (440) planes,[32] respectively. With the increase in reduction temperature, the peak belonging to Co_3O_4 became weaker, and diffraction relative to CoO and metallic Co was detected. The diffraction at $2\theta = 42.4°$ was assigned to the (200) plane of cubic phase CoO.

The Co/CoO_x samples at different reduction temperatures were tested using H_2-TPR. Prior to the TPR measurements, the catalysts were pre-treated, ensuring the absence of any organic or other residues. Clear H_2 consumption peaks were observed in the temperature ranges of 250–320 °C and 320–450 °C (Fig. S2†). The low-temperature peak corresponded to the reduction of Co^{3+} to Co^{2+} and the formation of CoO,[33] while the high-temperature peak corresponded to the reduction of Co^{2+} to metallic Co.[34] Previous studies reported the sequential reduction process that transitions from Co_3O_4 to CoO and subsequently to metallic Co.[35,36] The data delineated in Table 3 revealed that, among the catalyst specimens evaluated, Co/CoO_x-200 manifested the most substantial hydrogen uptake. As the reduction temperature increased, the amount of hydrogen consumption by the sample significantly decreased, confirming that a large amount of CoO_x in Co/CoO_x catalysts had been reduced. The amount of hydrogen consumption through the Co/CoO_x catalysts could be used to approximately calculate the proportion of Co in different valence states in the catalysts. The detailed results are shown in Table 3. The H_2-TPR outcomes substantiated the coexistence of CoO_x and metallic Co within the synthesized catalysts. The H_2-TPR outcomes were in agreement with those of XRD.

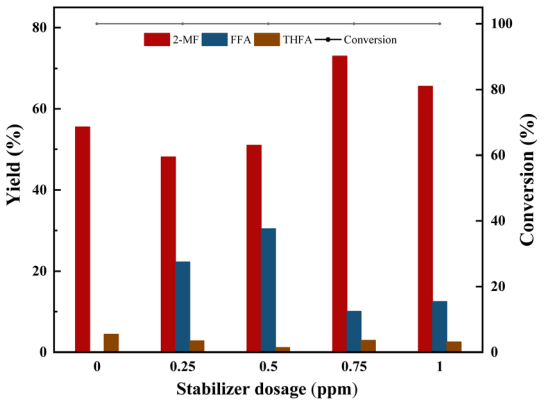

Fig. 4 Effect of stabilizer dosage on furfural selective hydrodeoxygenation conversion and yield using Co/CoO_x-300 catalysts. Reaction conditions: furfural 2 g, isopropyl 40 mL, catalyst 200 mg, temperature 170 °C, agitation speed 700 rpm, H_2 pressure 2 MPa, time 2 h. 2-MF: 2-methylfuran, FFA: furfuryl alcohol, THFA: tetrahydrofurfuryl alcohol.

3.2 Synthesis of 2-MF by furfural selective hydrodeoxygenation

The synthesis of 2MF was achieved through the selective hydrodeoxygenation of furfural using a high-pressure Parr reactor system. The selective hydrodeoxygenation procedure was executed under a hydrogen atmosphere for a duration of 2 h, utilizing the Co/CoO_x catalyst at its specified reduction temperature. This catalyst was synthesized by a straightforward precipitation technique, followed by a reduction process under 10% H_2 for 2 h. The literature review suggested that the synthesis of 2-MF *via* catalytic selective hydrodeoxygenation of furfural was initiated through the hydrogenation of its aldehyde functional group, yielding furfuryl alcohol. This was followed by the selective hydrodeoxygenation of the hydroxyl moiety in furfuryl alcohol to produce 2-MF. Nevertheless, during this latter stage of selective hydrodeoxygenation, there existed a proclivity for concurrent hydrogenation of the furan ring, culminating in the incidental generation of tetrahydrofurfuryl alcohol as an undesired byproduct.[37,38] Moreover, an elevated hydrogen pressure or a prolonged reaction duration could lead to the additional hydrogenation of the furan ring present in 2-MF, resulting in the formation of 2-methyltetrahydrofuran and 1,4-pentanediol. Simultaneously, the polymerization of furfural and furfuryl alcohol constituted prevalent presumable side reactions within this experimental framework. The aforementioned reaction sequence is delineated in Scheme 1.

3.2.1 Effect of reduction temperature. The reduction temperature of a catalyst could affect the extent of the catalyst's reduction, leading to changes in the catalyst's composition,

Table 4 Comparison of the hydrodeoxidation reaction with or without a catalyst[a]

Catalysts (g)	Reactant	Stabilizer dosage (ppm)	Conversion (%)	2-MF yield (%)	Furfuryl alcohol yield (%)	Polymer yield[b] (%)
0	Furfural	0	6	0	0	6
0	Furfuryl alcohol	0	11.4	0	0	11.4
0.2	Furfural	0	100	58	5	37
0.2	Furfuryl alcohol	0	15.1	10.3	0	4.8
0	Furfural	0.75	7	0	0	7
0.2	Furfural	0.75	100	73	11	16

[a] Reaction conditions: furfural 2 g, furfural alcohol 2 g isopropyl 40 mL, catalyst 200 mg, temperature 170 °C, agitation speed 700 rpm, H_2 pressure 2 MPa, time 2 h. 2-MF: 2-methylfuran. [b] The polymer yield was calculated by using the carbon balance, which was determined by subtracting the quantifiable amounts of reactants and products from 100%.

which in turn significantly impacts the performance of the catalyst (see Fig. 2). In the presence of a hydrogen atmosphere, the catalysts subjected to a range of temperatures (200 °C, 250 °C, 300 °C, and 350 °C) uniformly attained complete conversion of furfural, which substantiated the premise that the aldehyde moiety in furfural underwent facile hydrogenation in this reaction. Notably, the catalysts denoted as Co/CoO_x-250 and Co/CoO_x-300 demonstrated an enhanced selectivity towards the production of 2-MF. Conversely, the catalytic systems represented by Co/CoO_x-200 and Co/CoO_x-350 yielded a considerable quantity of furfuryl alcohol. This indicated that an excess of either metallic Co or CoO led to a decrease in the reactivity of furfuryl alcohol conversion into 2-MF. And it was exclusively the Co/CoO_x catalysts maintaining an optimal ratio of Co^0/Co^{2+} that demonstrated efficacious catalytic activity for cleaving the C–O bond in furfuryl alcohol, hence, attaining elevated selectivity for 2-MF. Drawing from the findings of Zhang *et al.*,[39] it was postulated that CoO played a role in adsorbing the furan ring, whereas the metallic Co was instrumental in facilitating the selective hydrodeoxygenation of aldehydic or hydroxylic functional groups. This synergistic interaction was imperative for achieving the maximal yield of 2-MF, thereby necessitating a judicious balance of Co and CoO within the catalytic framework.

3.2.2 Effect of reaction temperature. Fig. 3 delineates the influence of reaction temperature on the selectivity towards 2-MF. From Fig. 3, it was evident that the selectivity for 2-MF increased with the increase in reaction temperature. This phenomenon implied that the activation energy requisite for the selective hydrodeoxygenation of furfuryl alcohol to yield 2-MF surpasses that needed for the hydrogenation of the furan ring. Consequently, variations in temperature could more substantially accelerate the selective hydrodeoxygenation reaction, hence achieving high selectivity for the production of 2-MF at elevated temperatures. Prior research[40] has demonstrated that transition metal oxides, including CoO_x, exhibited efficacious catalysis in the cleavage of the C–O bond. Increasing the reaction temperature was favorable for Co and CoO to hydrogenize the C=O and C–O bonds, accelerating the reaction rate and promoting the generation of 2-MF.

3.2.3 Effect of hydroquinone dosage. By optimizing the catalyst and reaction parameters (see Fig. S3–S6†), a relatively high selectivity for 2-MF was attained, yet the carbon balance within the reaction system did not meet a satisfactory level. This suboptimal carbon balance was likely attributable to the undesired polymerization of furfural and furfuryl alcohol as side reactions. To mitigate these polymerization processes, hydroquinone, a polymerization inhibitor, was incorporated into the reaction solvent with the aim of enhancing the carbon balance of this reaction. Examination of Fig. 4 revealed that the addition of hydroquinone, even in minute concentrations, ameliorated the carbon balance. Specifically, the inclusion of 0.75 ppm hydroquinone resulted in a carbon balance of 86%, concurrently achieving a 73% yield of 2-MF. These findings suggested that hydroquinone was effective in substantially reducing the polymerization side reactions of furfural and furfuryl alcohol, thereby further improving the selectivity for 2-MF and carbon balance of the reaction.

To investigate the role of hydroquinone, three sets of comparative experiments were conducted. From Table 4, it can be observed that furfural underwent only minor polymerization reactions (6–7%) in the absence of a catalyst under the reaction conditions, and the addition of hydroquinone didnt inhibit this slight polymerization reaction. However, upon the addition of

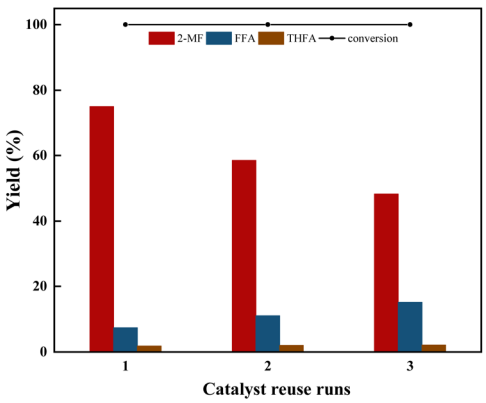

Fig. 5 Reusability of the catalyst for furfural selective hydrodeoxygenation conversion and yield using Co/CoO_x-300 catalysts. Reaction conditions: furfural 2 g, isopropyl 40 mL, catalyst 200 mg, stabilizer dosage 0.75 ppm, temperature 170 °C, agitation speed 700 rpm, H_2 pressure 2 MPa, time 2 h. 2-MF: 2-methylfuran, FFA: furfuryl alcohol, THFA: tetrahydrofurfuryl alcohol.

a Co-based catalyst, furfural underwent significant polymerization (37%). By adding hydroquinone, the polymerization reaction was significantly reduced to 16%, indicating that, in this process, the polymerization reaction was mainly due to the polymerization of furfural catalyzed by the Co-based catalyst.

Another particularly interesting phenomenon was observed with furfuryl alcohol, which behaved oppositely to furfural. In the absence of a catalyst, the polymerization was 11.4%. However, upon the addition of the catalyst, the polymerization decreased to 4.8%, indicating that the Co-based catalyst inhibited the polymerization of furfuryl alcohol. Consequently, it was feasible to delineate the reaction pathway for the selective hydrodeoxygenation of furfural into 2-MF by modulating the reaction selectivity. This involved consideration of side reactions, such as the polymerization of furfural and furfuryl alcohol, the reduction of furfuryl alcohol to tetrahydrofurfuryl alcohol, and the excessive hydrogenation of 2-MF resulting in the production of 2-methyltetrahydrofuran and 1,5-pentanediol. These processes are comprehensively illustrated in Scheme 1. Moreover, the observations from this study were in alignment with findings put forth by other researchers in this field.[41]

3.2.4 The recyclability of the catalyst. From Fig. 5, furfural was completely converted during three cycles of reuse experiments, indicating that the catalyst's hydrogenation ability remained intact. However, the selectivity towards the target product 2-MF noticeably decreased, while the selectivity towards the by-product THFA increased. Based on the results of N_2 physical adsorption and H_2-TPR of the used catalyst, it can be inferred that the decrease in catalyst selectivity towards 2-MF was primarily attributed to two aspects: changes in the physical structure and variations in the oxidation state of Co. After three cycles of the reaction, the catalyst's specific surface area decreased from 5.8 $m^2\ g^{-1}$ to 2.2 $m^2\ g^{-1}$, and the pore volume decreased from 0.0021 $cm^3\ g^{-1}$ to 0.0011 $cm^3\ g^{-1}$ (Table S2†). These findings indicated that during repeated use, the catalyst's pore structure collapsed or was blocked, resulting in decreased selectivity towards 2-MF. Table S3† shows the ratio of Co^0/Co^{2+} calculated based on H_2-TPR. It can be observed that during the reaction, some of the Co^{2+} was further reduced to Co^0, deviating from the optimal ratio of Co^0/Co^{2+} for achieving the highest 2-MF selectivity. This deviation led to a decrease in 2-MF selectivity. Meanwhile, we also conducted XRD characterization of the used catalyst (Fig. S7†). However, due to the low proportion of CoO, no significant changes were observed in the XRD pattern.

4 Conclusions

A collection of Co/CoO_x catalysts was synthesized *via* a simple precipitation technique, and their efficacy in catalyzing the selective hydrodeoxygenation of furfural to 2-MF was substantiated. In the series, Co/CoO_x-300 demonstrated superior selectivity towards the formation of 2-MF. The introduction of a small amount of hydroquinone, serving as a polymerization inhibitor, facilitated the attainment of 2-MF yields as high as 73% under mild reaction parameters (170 °C, 2 MPa H_2, for a duration of 2 hours) despite employing a substantial furfural/catalyst mass ratio of 10 : 1. Analytical techniques, including XRD and H_2-TPR ascertained that Co/CoO_x-300 predominantly consisted of metallic Co and CoO when the ratio of Co^0 to Co^{2+} within the catalyst was around 95% leading to optimal selectivity towards 2-MF. Conclusively, a mechanistic schematic delineating the selective hydrodeoxygenation of furfural to 2-MF was constructed, predicated on the observations gleaned from the experimental procedures (see Scheme 1).

Author contributions

Y. Han: conceptualization, methodology, investigation, writing – original draft, writing – review and editing. X. Zhang: methodology, investigation. W. Wang: data curation, methodology, investigation. S. Guo: methodology, investigation, writing – original draft, writing – review and editing. X. Ji: writing – review and editing, formal analysis. G. Li: writing – review and editing, formal analysis, project administration, funding acquisition.

Conflicts of interest

There are no conflicts of interest to declare.

Acknowledgements

We are grateful for the support from the National Natural Science Foundation of China (No. 22078318), and the Youth Innovation Promotion Association CAS (grant No. 2020186).

References

1 X. Wu, R. Daniel, G. Tian, H. Xu, Z. Huang and D. Richardson, *Appl. Energy*, 2011, **88**(7), 2305–2314.
2 D. M. Alonso, S. G. Wettstein and J. A. Dumesic, *Chem. Soc. Rev.*, 2012, **41**(24), 8075–8098.
3 Z. Zhang, J. Song and B. Han, *Chem. Rev.*, 2016, **117**(10), 6834–6880.
4 P. Gallezot, *Chem. Soc. Rev.*, 2012, **41**(4), 1538–1558.
5 A. S. Mamman, J. M. Lee, Y. C. Kim, I. T. Hwang, N. J. Park, Y. K. Hwang, J. S. Chang and J. S. Hwang, *Biofuels, Bioprod. Biorefin.*, 2008, **2**(5), 438–454.
6 J. J. Bozell and G. R. Petersen, *Green Chem.*, 2010, **12**(4), 539–554.
7 B. Wang, C. Li, B. He, J. Qi and C. Liang, *Energy Chem.*, 2017, **26**(4), 799–807.
8 P. Biswas, J. H. Lin, J. Kang and V. V. Guliants, *Appl. Catal., A*, 2014, **475**, 379–385.
9 X. Chang, A. F. Liu, B. Cai, J. Y. Luo, H. Pan and Y. B. Huang, *ChemSusChem*, 2016, **9**(23), 3330–3337.
10 B. J. Liu, L. H. Lu, B. C. Wang, T. X. Cai and I. Katsuyoshi, *Appl. Catal., A*, 1998, **171**(1), 117–122.
11 J. J. Musci, A. B. Merlo and M. L. Casella, *Catal. Today*, 2017, **296**, 43–50.
12 V. Vetere, A. B. Merlo, J. F. Ruggera and M. L. Casella, *J. Braz. Chem. Soc.*, 2010, **21**, 914–920.

13 Y. Román-Leshkov, C. J. Barrett, Z. Y. Liu and J. A. Dumesic, *Nature*, 2007, **447**(7147), 982–985.
14 G. Z. Ren, G. Y. Li, Y. Zhang, A. Q. Wang, X. D. Wang, Y. Cong, T. Zhang and N. Li, *Sustainable Energy Fuels*, 2022, **6**(4), 1156–1163.
15 M. Wu, T. Wang, W. H. Li, Q. Zhang, B. Zhang, K. Q. Chen, S. Y. Peng, G. J. Li, J. N. Huang, Q. Wang and C. Wang, *Chem. Eng. J.*, 2023, **461**, 141944.
16 J. G. M. Bremner and R. K. F. Keeys, *J. Chem. Soc.*, 1947, 1068–1080.
17 F. Ma, H. Li and J. Jiang, *Chem. Res. Chin. Univ.*, 2019, **35**(3), 498–503.
18 A. O'Driscoll, T. Curtin, W. Y. Hernández, P. Van Der Voort and J. J. Leahy, *Org. Process Res. Dev.*, 2016, **20**(11), 1917–1929.
19 O. F. Aldosari, S. Iqbal, P. J. Miedziak, G. L. Brett, D. R. Jones, X. Liu, J. K. Edwards, D. J. Morgan, D. K. Knight and G. J. Hutchings, *Catal. Sci. Technol.*, 2016, **6**(1), 234–242.
20 P. Panagiotopoulou, N. Martin and D. G. Vlachos, *J. Mol. Catal. A: Chem.*, 2014, **392**, 223–228.
21 N. S. Date, A. M. Hengne, K. W. Huang, R. C. Chikate and C. V. Rode, *Green Chem.*, 2018, **20**(9), 2027–2037.
22 C. Xu, L. Zheng, D. Deng, J. Liu and S. Liu, *Catal. Commun.*, 2011, **12**(11), 996–999.
23 M. Kalong, P. Hongmanorom, S. Ratchahat, W. Kooamornpattana, K. Faungnawakij, S. Assabumrungrat, A. Srifa and S. Kawi, *Fuel Process. Technol.*, 2021, **214**, 106721.
24 W. b. Gong, C. Chen, H. Zhang, G. Wang and H. Zhao, *ChemistrySelect*, 2017, **2**(31), 9984–9991.
25 H. Li, H. Liu, C. Cai, H. Wang, Y. Huang, S. Li, B. Yang, C. Wang, Y. Liao and L. Ma, *Catal. Commun.*, 2023, **175**, 106625.
26 S. Akmaz, S. Algorabi and S. N. Koc, *Can. J. Chem. Eng.*, 2021, **99**, S562–S574.
27 Z. Zhang, Z. Zhang, X. Zhang, F. Wang, Z. Wang, Y. Li, X. Wang, R. Ahishakiye and X. Zhang, *Appl. Surf. Sci.*, 2023, **612**, 155871.
28 Y. An, Q. Wu, L. Niu, C. Zhang, Q. Liu, G. Bian and G. Bai, *J. Catal.*, 2024, **429**, 115271.
29 S. Xiang, L. Dong, Z. Q. Wang, X. Han, L. L. Daemen, J. Li, Y. Q. Cheng, Y. Guo, X. H. Liu, Y. F. Hu, A. J. Ramirez-Cuesta, S. H. Yang, X. Q. Gong and Y. Q. Wang, *Nat. Commun.*, 2022, **13**(1), 3657.
30 J. Zhu, F. Q. Chen, Z. G. Zhang, M. Li, Q. W. Yang, Y. W. Yang, Z. B. Bao and Q. L. Ren, *ACS Sustain. Chem. Eng.*, 2019, **7**(15), 12955–12963.
31 A. Takagaki, M. Ohara, S. Nishimura and K. Ebitani, *Chem. Commun.*, 2009, **41**, 6276–6278.
32 H. Wu, G. Pantaleo, G. Di Carlo, S. Guo, G. Marcì, P. Concepción, A. M. Venezia and L. F. Liotta, *Catal. Sci. Technol.*, 2015, **5**(3), 1888–1901.
33 W. P. Ma, Y. J. Ding and L. W. Lin, *Ind. Eng. Chem. Res.*, 2004, **43**(10), 2391–2398.
34 S. R. De Miguel, M. C. Rom n-Martınez, E. L. Jablonski, J. L. G. Fierro, D. Cazorla-Amorós and O. A. Scelza, *J. Catal.*, 1999, **184**(2), 514–525.
35 W. Chu, P. Chernavskii, L. Gengembre, G. Pankina, P. Fongarland and A. Khodakov, *J. Catal.*, 2007, **252**(2), 215–230.
36 B. Solsona, T. E. Davies, T. Garcia, I. Vázquez, A. Dejoz and S. H. Taylor, *Appl. Catal., B*, 2008, **84**(1–2), 176–184.
37 P. Koley, S. Chandra Shit, B. Joseph, S. Pollastri, Y. M. Sabri, E. L. H. Mayes, L. Nakka, J. Tardio and J. Mondal, *ACS Appl. Mater. Interfaces*, 2020, **12**(19), 21682–21700.
38 T. Varila, E. Mäkelä, R. Kupila, H. Romar, T. Hu, R. Karinen, L. R. Puurunen and U. Lassi, *Catal. Today*, 2021, **367**, 16–27.
39 Z. L. Zhang, Z. W. Zhang, X. B. Zhang, F. M. Wang, Z. Wang, Y. W. Li, X. T. Wang, R. Ahishakiye and X. Zhang, *Appl. Surf. Sci.*, 2023, **612**, 155871.
40 K. Yan, G. Wu, T. Lafleur and C. Jarvis, *Renewable Sustainable Energy Rev.*, 2014, **38**, 663–676.
41 S. Liu, Y. Amada, M. Tamura, Y. Nakagawa and K. Tomishige, *Green Chem.*, 2014, **16**(2), 617–626.
42 X. Gong, N. Li, Y. Li and R. Hu, *Mol. Catal.*, 2022, **531**, 112651.
43 S. Srivastava, G. C. Jadeja and J. Parikh, *Chem. Eng. Res. Des.*, 2018, **132**, 313–324.
44 P. Bretzler, M. Huber, S. Nickl and K. Köhler, *RSC Adv.*, 2020, **10**(46), 27323–27330.